

# Suppression of spin-density-wave transition and emergence of ferromagnetic ordering of $\text{Eu}^{2+}$ moments in $\text{EuFe}_{2-x}\text{Ni}_x\text{As}_2$

Zhi Ren, Xiao Lin, Qian Tao, Shuai Jiang, Zengwei Zhu, Cao Wang, Guanghan Cao,\* and Zhu'an Xu†  
*Department of Physics, Zhejiang University, Hangzhou 310027, China*

(Received 13 November 2008; revised manuscript received 25 February 2009; published 27 March 2009)

We present a systematic study on the physical properties of  $\text{EuFe}_{2-x}\text{Ni}_x\text{As}_2$  ( $0 \leq x \leq 0.2$ ) by electrical resistivity, magnetic susceptibility, and thermopower measurements. The undoped compound  $\text{EuFe}_2\text{As}_2$  undergoes a spin density wave (SDW) transition associated with Fe moments at 195 K, followed by antiferromagnetic (AFM) ordering of  $\text{Eu}^{2+}$  moments at 20 K. Ni doping at the Fe site simultaneously suppresses the SDW transition and AFM ordering of  $\text{Eu}^{2+}$  moments. For  $x \geq 0.06$ , the magnetic ordering of  $\text{Eu}^{2+}$  moments evolves from antiferromagnetic to ferromagnetic (FM). The SDW transition is completely suppressed for  $x \geq 0.16$ , however, no superconducting transition was observed down to 2 K. The possible origins of the AFM-to-FM transition and the absence of superconductivity in the  $\text{EuFe}_{2-x}\text{Ni}_x\text{As}_2$  system are discussed.

DOI: [10.1103/PhysRevB.79.094426](https://doi.org/10.1103/PhysRevB.79.094426)

PACS number(s): 75.30.Fv, 75.50.-y, 75.60.Ej

## I. INTRODUCTION

The discovery of superconductivity up to 56 K in iron-based arsenides<sup>1-7</sup> has aroused great interest in the community of condensed-matter physics. The undoped parent compounds adopt the tetragonal structure at room temperature, which consists of  $[\text{Fe}_2\text{As}_2]^{2-}$  layers separated alternatively by  $[\text{Ln}_2\text{O}_2]^{2+}$  (Refs. 8 and 9) or  $A^{2+}$  ( $A=\text{Ca}, \text{Sr}, \text{Ba}, \text{Eu}$ ) layers.<sup>10-13</sup> At low temperatures, the parent compounds undergo a structural phase transition from tetragonal to orthorhombic, accompanied<sup>14</sup> or followed<sup>15</sup> by a SDW-like antiferromagnetic (AFM) phase transition. Doping with electrons or holes in the parent compounds suppresses the phase transitions and induces the high temperature superconductivity. This intimate connection between superconductivity and magnetism suggests unconventional superconductivity in the iron-based arsenides.<sup>16-18</sup>

Very recently, superconductivity has been observed in  $\text{LaFe}_{1-x}\text{M}_x\text{AsO}$ <sup>19-21</sup> and  $\text{BaFe}_{2-x}\text{M}_x\text{As}_2$ <sup>22,23</sup> ( $M=\text{Co}$  and  $\text{Ni}$ ). These findings are quite remarkable and challenge our common wisdom of superconductivity, which shows that direct doping in the superconducting-active blocks generally destroys superconductivity. In high- $T_c$  cuprates, actually, Ni substitution for Cu in the  $\text{CuO}_2$  planes drastically reduces  $T_c$ . Hence these experimental results provide clues to the superconducting mechanism for the iron-based arsenide superconductors. Currently, an itinerant scenario within rigid band model is more favored to understand this unusual doping-induced superconductivity.<sup>24</sup>

$\text{EuFe}_2\text{As}_2$  is a unique member in the ternary iron arsenide family due to the fact that  $\text{Eu}^{2+}$  ions carry local moments, which order antiferromagnetically below 20 K.<sup>12,25,26</sup> Except this AFM transition, the physical properties of  $\text{EuFe}_2\text{As}_2$  were found to be quite similar with those of its isostructural compounds  $\text{BaFe}_2\text{As}_2$  and  $\text{SrFe}_2\text{As}_2$ ,<sup>25</sup> both of which become superconducting upon appropriate doping.<sup>27-29</sup> It was then expected that  $\text{EuFe}_2\text{As}_2$  could be tuned superconducting through similar doping strategies. Indeed, superconductivity with  $T_c$  over 30 K has been observed in  $(\text{Eu}, \text{K})\text{Fe}_2\text{As}_2$  (Ref. 30) and  $(\text{Eu}, \text{Na})\text{Fe}_2\text{As}_2$ .<sup>31</sup>

Doping at the Fe site in  $\text{EuFe}_2\text{As}_2$  takes advantage of inducing possible superconductivity while leaving the mag-

netic  $\text{Eu}^{2+}$  layers intact, which could provide us insight to the interplay between superconductivity and magnetism. Here we report a systematic study on the physical properties in  $\text{EuFe}_{2-x}\text{Ni}_x\text{As}_2$  ( $0 \leq x \leq 0.2$ ) system. It was found that both the SDW ordering of Fe moments and the AFM ordering of  $\text{Eu}^{2+}$  moments were suppressed by substituting Fe with Ni. Ferromagnetic (FM) ordering of  $\text{Eu}^{2+}$  moments emerges for  $x \geq 0.06$ . While the SDW transition is completely suppressed for  $x \geq 0.16$ , no superconducting transition was observed down to 2 K in  $\text{EuFe}_{2-x}\text{Ni}_x\text{As}_2$ , in contrast with the superconductivity in  $\text{BaFe}_{2-x}\text{Ni}_x\text{As}_2$ .<sup>23</sup> Our results suggest a strong coupling between the magnetism of  $\text{Eu}^{2+}$  ions and the conduction electrons of  $[\text{Fe}_{2-x}\text{Ni}_x\text{As}_2]^{2-}$  layers.

## II. EXPERIMENT

Polycrystalline samples of  $\text{EuFe}_{2-x}\text{Ni}_x\text{As}_2$  ( $x=0, 0.03, 0.06, 0.09, 0.12, 0.16, \text{ and } 0.2$ ) were synthesized by solid-state reaction with  $\text{EuAs}$ ,  $\text{Fe}_2\text{As}$  and  $\text{Ni}_2\text{As}$ .  $\text{EuAs}$  was presynthesized by reacting Eu grains and As powders in evacuated silica tube at 873 K for 10 h then 1123 K for 36 h.  $\text{Fe}_2\text{As}$  was presynthesized by reacting Fe powers and As powders at 873 K for 10 h and 1173 K for 2.5 h.  $\text{Ni}_2\text{As}$  was presynthesized by reacting Ni powders and As powders at 873 K for 10 h then 1073 K for another 10 h. The powders of  $\text{EuAs}$ ,  $\text{Fe}_2\text{As}$ , and  $\text{Ni}_2\text{As}$  were weighed according to the stoichiometric ratio, thoroughly ground and pressed into pellets in an argon-filled glove box. The pellets were sealed in evacuated quartz tubes and annealed at 1173 K for 24 h and furnace-cooled to room temperature. Powder x-ray diffraction (XRD) was performed at room temperature using a D/Max-rA diffractometer with  $\text{Cu K}\alpha$  radiation and a graphite monochromator. The data were collected with a step-scan mode. The structural refinements were performed using the program RIETAN 2000.<sup>32</sup> The electrical resistivity was measured using a standard four-probe method. The measurements of dc magnetic properties were performed on a quantum design magnetic property measurement system (MPMS-5). Thermopower measurements were carried out in a cryogenic refrigerator down to 17 K by a steady-state technique with a temperature gradient  $\sim 1$  K/cm.

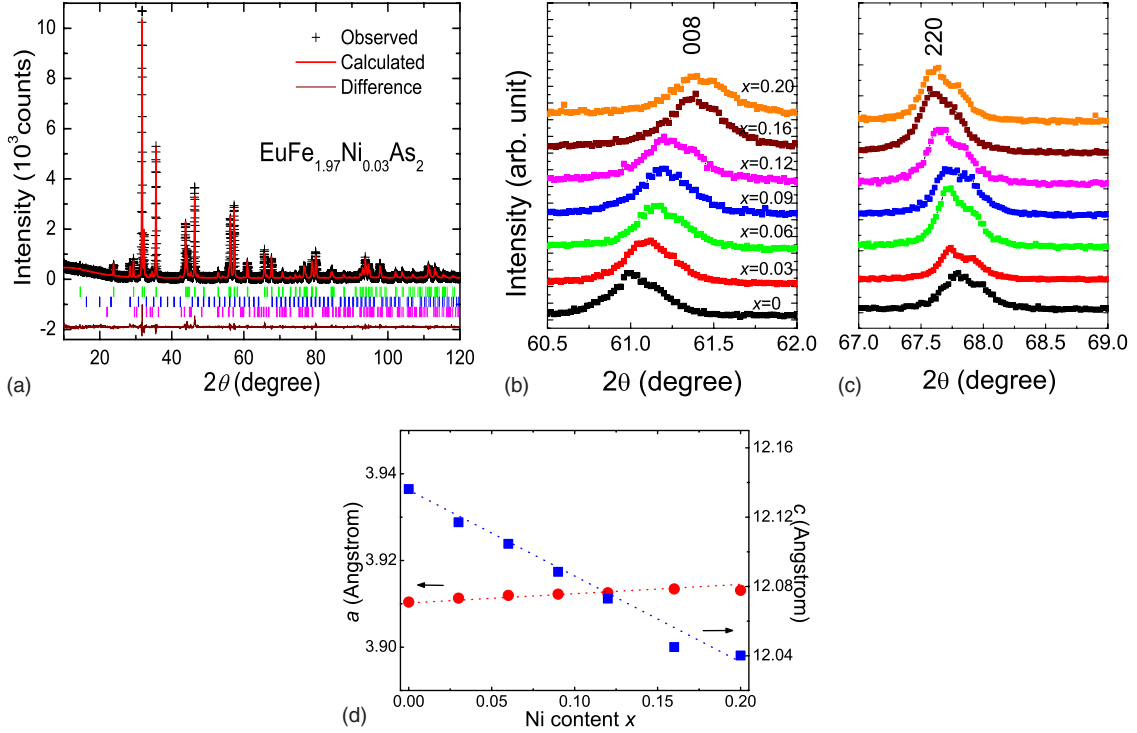


FIG. 1. (Color online) (a) X-ray powder diffraction pattern at room temperature and the Rietveld refinement profile for the  $\text{EuFe}_{1.97}\text{Ni}_{0.03}\text{As}_2$  sample.  $\text{Eu}_2\text{O}_3$  ( $\sim 1.4\%$ ) and  $\text{Fe}_{0.985}\text{Ni}_{0.015}\text{As}$  ( $\sim 6\%$ ) are also included in the refinement. (b) and (c) represent the (008) and (220) diffraction peaks for the  $\text{EuFe}_{2-x}\text{Ni}_x\text{As}_2$  samples, respectively. (d) Refined lattice parameters plotted as functions of Ni content  $x$ .

### III. RESULTS AND DISCUSSION

The crystal structure for all the  $\text{EuFe}_{2-x}\text{Ni}_x\text{As}_2$  ( $x = 0, 0.03, 0.06, 0.09, 0.12, 0.16, 0.2$ ) samples at room temperature was refined with the tetragonal  $\text{ThCr}_2\text{Si}_2$  structure. An example of the refinement profile for  $\text{EuFe}_{1.97}\text{Ni}_{0.03}\text{As}_2$  is shown in Fig. 1(a). The weighted pattern factor and goodness of fit are  $R_{\text{wp}} \sim 11.2\%$  and  $S \sim 1.6$ , indicating a fairly good refinement. Minor impurity phases of  $\text{Eu}_2\text{O}_3$  and  $\text{Fe}_{0.985}\text{Ni}_{0.015}\text{As}$  are also identified. In addition, the refined occupancies are close to the nominal value. With increasing Ni content, the (008) diffraction peaks shift toward higher angles [Fig. 1(b)] while the (220) diffraction peaks shift toward lower angles [Fig. 1(c)]. This observation is consistent with the result from the Rietveld refinements, which show that  $a$  axis increases slightly while  $c$  axis shrinks remarkably with increasing Ni content, as shown in Fig. 1(d).

Figure 2 shows the temperature dependence of resistivity ( $\rho$ ) for the  $\text{EuFe}_{2-x}\text{Ni}_x\text{As}_2$  samples. The  $\rho$  value at 300 K decreases with increasing Ni content, which is probably attributed to the increase of carrier concentration induced by the Ni doping. For the parent compound,  $\rho$  drops rapidly below 195 K and shows a kink at  $\sim 20$  K. The former is associated with a SDW transition of Fe moments while the latter is due to the AFM ordering of  $\text{Eu}^{2+}$  moments.<sup>25</sup> On Ni doping, the anomaly in  $\rho$  associated with the SDW transition is presented as an upturn, followed by a hump. This behavior resembles that observed in  $\text{BaFe}_{2-x}\text{Ni}_x\text{As}_2$  crystals.<sup>23</sup> With increasing Ni content  $x$ ,  $T_{\text{SDW}}$  shifts to lower temperatures. For  $x \geq 0.16$  the SDW transition is completely suppressed, however, no superconducting transition was observed down

to the lowest temperature in the present study. Instead, two kinks in  $\rho$  at low temperatures are present, which can be seen more clearly in the derivative plots as shown in the inset of Fig. 2. It is probable that they share the same origin as that of undoped  $\text{EuFe}_2\text{As}_2$  under magnetic fields, which is related to the different magnetic states of  $\text{Eu}^{2+}$  moments.<sup>33</sup>

Figure 3 shows the temperature dependence of thermopower ( $S$ ) for  $\text{EuFe}_{2-x}\text{Ni}_x\text{As}_2$  samples. The sign reversal behavior, which manifests multiband scenario, is observed for  $x=0$  and 0.03. The value of  $S$  for the other samples is negative. With increasing Ni content, the room-temperature thermopower is pushed toward more negative values, as

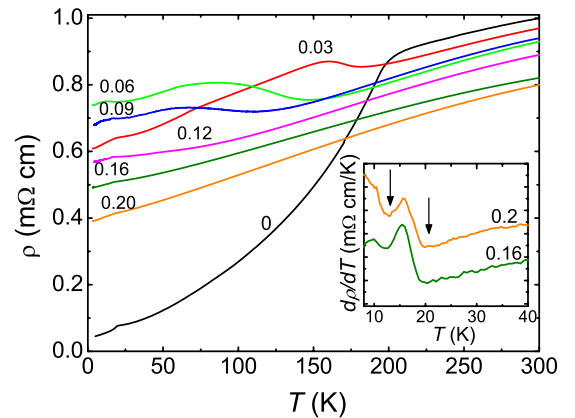


FIG. 2. (Color online) Temperature dependence of resistivity for the  $\text{EuFe}_{2-x}\text{Ni}_x\text{As}_2$  samples. The inset shows derivative plots for  $x=0.16$  and 0.2 below 40 K. The anomalies are marked by arrows.

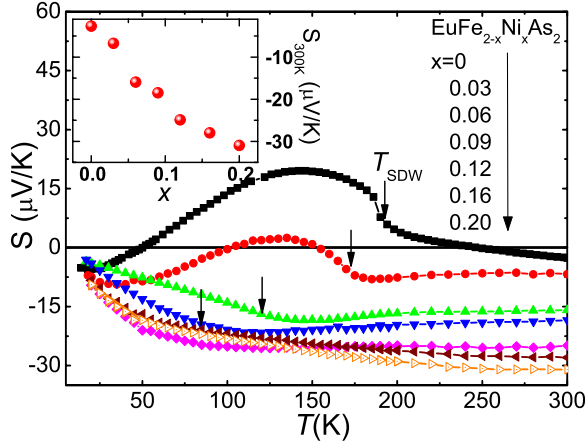


FIG. 3. (Color online) Temperature dependence of thermopower for the  $\text{EuFe}_{2-x}\text{Ni}_x\text{As}_2$  samples. The inset shows the thermopower value at 300 K plotted as a function of Ni content  $x$ .

shown in the inset of Fig. 3. For a simple two-band model with electrons and holes,  $S$  can be expressed as

$$S = \frac{n_h \mu_h |S_h| - n_e \mu_e |S_e|}{n_h \mu_h + n_e \mu_e}, \quad (1)$$

where  $n_{h(e)}$ ,  $\mu_{h(e)}$ , and  $|S_{h(e)}|$  denote the concentration, mobility and thermopower contribution of the holes (electrons), respectively. Therefore, the increase in  $|S|$  suggests that Ni doping increases the electron concentration. Meanwhile, the anomaly due to the SDW transition is suppressed to lower temperatures and is no longer visible for  $x=0.16$ , in agreement with the above resistivity measurements. Recently, it was found that there exists enhanced thermopower in the superconducting window of  $\text{SmFe}_{1-x}\text{Co}_x\text{AsO}$  system.<sup>20</sup> In the present system, no such enhancement was observed, which may be related to the absence of superconductivity.

Figure 4(a) shows the temperature dependence of magnetic susceptibility ( $\chi$ ) for the  $\text{EuFe}_{2-x}\text{Ni}_x\text{As}_2$  samples below 40 K under an applied field of 20 Oe. The  $\chi$  data of  $25 \leq T \leq 180$  K for  $x \geq 0.03$  basically fall onto the same curve, which can be well fitted by the modified Curie-Weiss law,

$$\chi = \chi_0 + \frac{C}{T - \theta}, \quad (2)$$

where  $\chi_0$  denotes the temperature-independent term,  $C$  as the Curie-Weiss constant, and  $\theta$  as the paramagnetic Curie temperature. The refined parameters are  $C=8.0(1)$  emu K/mol and  $\theta=19(1)$  K. The calculated effective moment  $P_{\text{eff}}$  is  $\sim 8\mu_B$  per formula unit, close to the theoretical value of  $7.94\mu_B$  for a free  $\text{Eu}^{2+}$  ion. It is evident that the valence state of Eu ions remains +2 and ferromagnetic interaction between  $\text{Eu}^{2+}$  moments dominates up to 10% Ni doping. The anomaly in susceptibility due to the SDW transition is hardly observed even after subtracting the Curie-Weiss contribution of  $\text{Eu}^{2+}$  moments. On further cooling, a sharp peak can be observed in both  $\chi_{\text{ZFC}}$  and  $\chi_{\text{FC}}$  for  $x=0.03$  at  $\sim 19$  K, similar to that observed in undoped  $\text{EuFe}_2\text{As}_2$ .<sup>25</sup> We ascribe this peak to the AFM ordering of  $\text{Eu}^{2+}$  moments. With increasing Ni content to 0.06, the peak shifts to  $\sim 16$  K. Surprisingly, for the same sample, a small bifurcation between zero-field-cooling (ZFC) and field-cooling (FC) curves develops below  $\sim 13$  K, suggesting the formation of ferromagnetic domains. For  $x \geq 0.09$ , an obvious divergence between  $\chi_{\text{ZFC}}$  and  $\chi_{\text{FC}}$  is seen, suggesting the emergence of FM ordered state. It is also noted that there exists a broad peak below  $T_{\text{Curie}}$  in the ZFC curves for  $x \geq 0.12$ . Interestingly,  $T_{\text{Curie}}$  and  $T_{\text{peak}}$  coincide with aforementioned two kinks in  $\rho$  at low temperatures, respectively. In  $\text{EuFe}_2\text{As}_2$  single crystals, we have observed a metamagnetic phase with applied field perpendicular to the  $c$  axis.<sup>33</sup> Thus we speculate that  $T_{\text{peak}}$  may be related to a successive metamagnetic transition.

Figure 4(b) shows the field dependence of magnetization for the  $\text{EuFe}_{2-x}\text{Ni}_x\text{As}_2$  samples at 2 K. For  $x=0.03$ , a slope change in the  $M$ - $H$  curve can be seen clearly at  $\mu_0 H = 0.55$  T, which is ascribed to a field-induced metamagnetic transition.<sup>25,33,34</sup> Moreover, there is no hysteresis loop in the low field region, consistent with the AFM ground state of  $\text{Eu}^{2+}$  moments. For the other samples, however,  $M$  increases steeply with initial increasing  $H$ . In addition, small hysteresis loops are observed. These results are in agreement with the above susceptibility measurements, suggesting that  $\text{Eu}^{2+}$  moments are FM ordered for  $x \geq 0.06$ . It is noted that all the

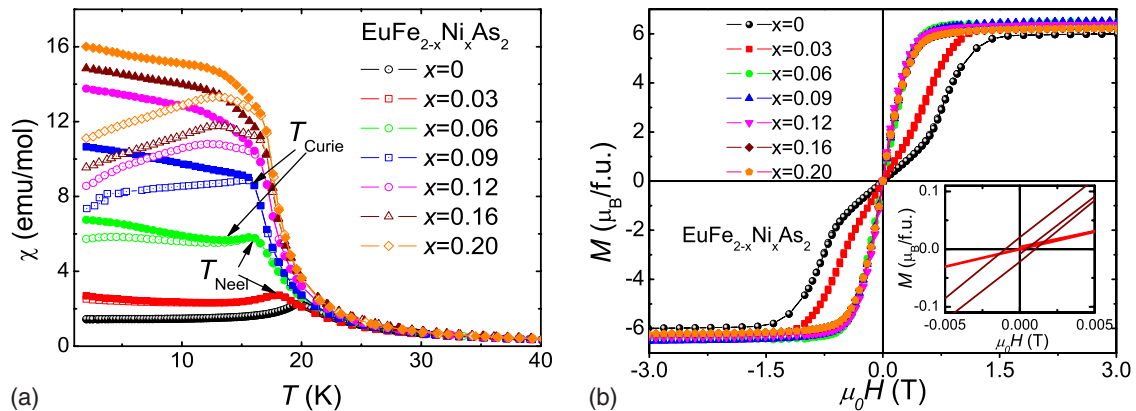


FIG. 4. (Color online) (a) Temperature dependence of ZFC (open symbols) and FC (solid symbols) magnetic susceptibility for the  $\text{EuFe}_{2-x}\text{Ni}_x\text{As}_2$  samples. (b) Field dependence of magnetization at 2 K for the  $\text{EuFe}_{2-x}\text{Ni}_x\text{As}_2$  samples. The inset shows an expanded plot of the low field region for  $x=0.03$  and 0.16.

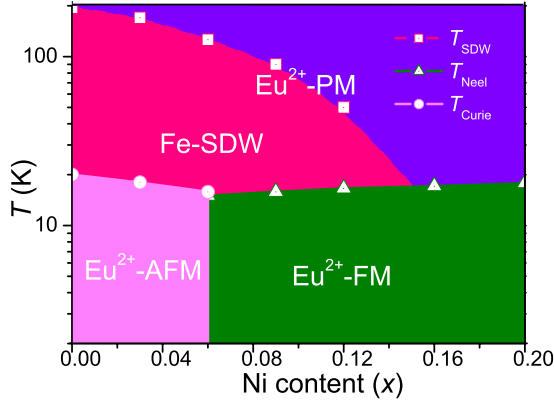


FIG. 5. (Color online) Magnetic phase diagram for  $\text{EuFe}_{2-x}\text{Ni}_x\text{As}_2$  system ( $0 \leq x \leq 0.2$ ).

saturated magnetic moments are around  $6.3\mu_B$  per formula, which is smaller than the theoretical value of  $7\mu_B$  for a free  $\text{Eu}^{2+}$  ion. This discrepancy is attributed to presence of impurity phases, whose magnetic response is much weaker.

Our experimental results on the physical properties of the  $\text{EuFe}_{2-x}\text{Ni}_x\text{As}_2$  system are summarized in the magnetic phase diagram in Fig. 5. The parent compound  $\text{EuFe}_2\text{As}_2$  shows AFM ordering of  $\text{Eu}^{2+}$  moments at 20 K as well as SDW ordering of Fe moments at 195 K. With Ni doping, both the orderings are suppressed. On one hand, the SDW transition is gradually suppressed and eventually disappears at  $x = 0.16$ . Nevertheless, no superconductivity was observed down to 2 K. On the other hand, the magnetic ordering of  $\text{Eu}^{2+}$  moments changes from AFM to FM at  $x \approx 0.06$ . This observation is surprising in view of the AFM ordering of  $\text{Eu}^{2+}$  moments in both the end members  $\text{EuFe}_2\text{As}_2$  and  $\text{EuNi}_2\text{As}_2$ .<sup>35</sup> By contrast,  $T_{\text{Neel}}$  remains nearly unchanged upon 10% Fe doping in  $\text{EuNi}_2\text{As}_2$ .<sup>36</sup>

The AFM structure of  $\text{Eu}^{2+}$  moments in  $\text{EuFe}_2\text{As}_2$  is proposed to be of A-type, i.e., FM coupling for intralayer  $\text{Eu}^{2+}$  moments while AFM coupling for interlayer  $\text{Eu}^{2+}$  moments.<sup>25,33,34</sup> The distance between nearest  $\text{Eu}^{2+}$  layers is  $\sim 6$  Å hence direct overlap of interlayer Eu 4f orbitals can be neglected. Therefore, the AFM exchange between interlayer  $\text{Eu}^{2+}$  moments is probably ascribed to the carrier-mediated Ruderman-Kittel-Kasuya-Yosida (RKKY) interaction.<sup>35</sup> The RKKY exchange coupling  $J_{\text{RKKY}} \propto -\frac{\alpha \cos \alpha - \sin \alpha}{\alpha^4}$ , where  $\alpha = 2k_F R$ ,  $R$  denotes the distance between two magnetic moments and  $k_F$  the Fermi vector. One can see that  $J_{\text{RKKY}}$  oscillates between AFM (negative) and FM (positive) at the variation of  $2k_F R$ . Considering the dimensionality of the Fermi surfaces, it is probably that heavy three-dimensional (3D) hole pocket derived from Fe  $d_z$  states<sup>18</sup> is responsible for mediating the RKKY interaction. Substitution of Fe with Ni introduces electrons, which results in the decrease in  $k_F^z$ . Meanwhile,  $R$  is also shortened, as indicated by the reduction in  $c$  axis. Thus the interlayer coupling may be

tuned from AFM to FM. On the other hand, the FM interaction within the  $\text{Eu}^{2+}$  layers persists up to 10% Ni doping. As a consequence, a FM ordering of  $\text{Eu}^{2+}$  moments is established. In contrast, the dominant interaction between  $\text{Eu}^{2+}$  moments in  $\text{EuNi}_2\text{As}_2$  is antiferromagnetic, as indicated by negative paramagnetic Curie temperature.<sup>35</sup> This may account for the robust AFM ordering of  $\text{Eu}^{2+}$  moments upon Fe doping in  $\text{EuNi}_2\text{As}_2$ . The clarification of these issues relies on further angle resolved photoemission spectroscopy (ARPES) as well as neutron-diffraction studies.

In the iron-based arsenides, superconductivity generally emerges as the SDW order is suppressed by the carrier doping. As a matter of fact, superconductivity with the maximum  $T_c$  of  $\sim 20$  K has been observed in  $\text{BaFe}_{2-x}\text{Ni}_x\text{As}_2$  system.<sup>23</sup> Thus, the absence of superconductivity in  $\text{EuFe}_{2-x}\text{Ni}_x\text{As}_2$  may be relevant to the magnetism of  $\text{Eu}^{2+}$  ions. The RKKY interaction mentioned above may hinder the Cooper pairing for superconductivity. Recently, reentrant superconducting behavior has been observed in a high pressure study of  $\text{EuFe}_2\text{As}_2$  crystal.<sup>37</sup> The results suggest that once  $T_c$  becomes smaller than the magnetic ordering temperature of  $\text{Eu}^{2+}$  moments, superconductivity will be completely suppressed. If  $\text{EuFe}_{2-x}\text{Ni}_x\text{As}_2$  were superconducting, its maximum  $T_c$  would be  $\sim 6$  K smaller than that of  $\text{BaFe}_{2-x}\text{Ni}_x\text{As}_2$  due to the existence of paramagnetic  $\text{Eu}^{2+}$  ions.<sup>37</sup> The assumed  $T_c$  is below the Curie temperatures. This could account for the absence of superconductivity in  $\text{EuFe}_{2-x}\text{Ni}_x\text{As}_2$  system.

#### IV. CONCLUSION

In summary, we have systematically studied the transport and magnetic properties on a series of  $\text{EuFe}_{2-x}\text{Ni}_x\text{As}_2$  polycrystalline samples with  $0 \leq x \leq 0.2$ . It is found that both the SDW transition associated with the Fe moments and the AFM ordering of  $\text{Eu}^{2+}$  moments are suppressed upon Ni doping. Though the SDW transition is completely suppressed for  $x \geq 0.16$ , no superconducting transition is observed down to 2 K. Surprisingly, a FM ground state of  $\text{Eu}^{2+}$  moments emerges for  $x \geq 0.06$ . A detailed magnetic phase diagram is presented and discussed within the RKKY framework. Our results suggest there exists a strong coupling between the magnetism of  $\text{Eu}^{2+}$  ions and the electronic state in the  $[\text{Fe}_{2-x}\text{Ni}_x\text{As}_2]^{2-}$  layers.

#### ACKNOWLEDGMENTS

We would like to thank J. H. Dai and Q. Si for helpful discussions. This work is supported by the National Basic Research Program of China (under Contracts No. 2006CB601003 and No. 2007CB925001) and the PCSIRT of the Ministry of Education of China (under Contract No. IRT0754).

\*ghcao@zju.edu.cn

†zhuan@zju.edu.cn

- <sup>1</sup>Y. Kamihara, T. Watanabe, M. Hirano, and H. Hosono, *J. Am. Chem. Soc.* **130**, 3296 (2008).
- <sup>2</sup>X. H. Chen, T. Wu, G. Wu, R. H. Liu, H. Chen, and D. F. Fang, *Nature (London)* **453**, 761 (2008).
- <sup>3</sup>G. F. Chen, Z. Li, D. Wu, G. Li, W. Z. Hu, J. Dong, P. Zheng, J. L. Luo, and N. L. Wang, *Phys. Rev. Lett.* **100**, 247002 (2008).
- <sup>4</sup>Z. A. Ren, J. Yang, W. Lu, W. Yi, G. C. Che, X. L. Dong, L. L. Sun, and Z. X. Zhao, *Mater. Res. Innovations* **12**, 105 (2008).
- <sup>5</sup>Z. A. Ren, J. Yang, W. Lu, W. Yi, X. L. Shen, Z. C. Li, G. C. Che, X. L. Dong, L. L. Sun, F. Zhou, and Z. X. Zhao, *EPL* **82**, 57002 (2008).
- <sup>6</sup>H. H. Wen, G. Mu, L. Fang, H. Yang, and X. Y. Zhu, *EPL* **82**, 17009 (2008).
- <sup>7</sup>C. Wang, L. J. Li, S. Chi, Z. W. Zhu, Z. Ren, Y. K. Li, Y. T. Wang, X. Lin, Y. K. Luo, S. Jiang, X. F. Xu, G. H. Cao, and Z. A. Xu, *EPL* **83**, 67006 (2008).
- <sup>8</sup>V. Johnson and W. Jeitschko, *J. Solid State Chem.* **11**, 161 (1974).
- <sup>9</sup>P. Quebe, L. J. Terbüchte, and W. Jeitschko, *J. Alloys Compd.* **302**, 70 (2000).
- <sup>10</sup>M. Pfisterer and G. Nagorsen, *Z. Naturforsch. B* **35B**, 703 (1980).
- <sup>11</sup>M. Pfisterer and G. Nagorsen, *Z. Naturforsch. B* **38B**, 811 (1983).
- <sup>12</sup>R. Marchand and W. Jeitschko, *J. Solid State Chem.* **24**, 351 (1978).
- <sup>13</sup>G. Wu, H. Chen, T. Wu, Y. L. Xie, Y. J. Yan, R. H. Liu, X. F. Wang, J. J. Ying, and X. H. Chen, *J. Phys.: Condens. Matter* **20**, 422201 (2008).
- <sup>14</sup>M. Rotter, M. Tegel, D. Johrendt, I. Schellenberg, W. Hermes, and R. Pöttgen, *Phys. Rev. B* **78**, 020503(R) (2008).
- <sup>15</sup>C. de la Cruz, Q. Huang, J. W. Lynn, J. Li, W. Ratcliff II, H. A. Mook, G. F. Chen, J. L. Luo, N. L. Wang, and Pengcheng Dai, *Nature (London)* **453**, 899 (2008).
- <sup>16</sup>K. Haule, J. H. Shim, and G. Kotliar, *Phys. Rev. Lett.* **100**, 226402 (2008).
- <sup>17</sup>C. Cao, P. J. Hirschfeld, and H. P. Cheng, *Phys. Rev. B* **77**, 220506(R) (2008).
- <sup>18</sup>D. J. Singh and M. H. Du, *Phys. Rev. Lett.* **100**, 237003 (2008).
- <sup>19</sup>A. S. Sefat, A. Huq, M. A. McGuire, R. Jin, B. C. Sales, D. Mandrus, L. M. D. Cranswick, P. W. Stephens, and K. H. Stone, *Phys. Rev. B* **78**, 104505 (2008).
- <sup>20</sup>C. Wang, Y. K. Li, Z. W. Zhu, S. Jiang, X. Lin, Y. K. Luo, S. Chi, L. J. Li, Z. Ren, M. He, H. Chen, Y. T. Wang, Q. Tao, G. H. Cao, and Z. A. Xu, *Phys. Rev. B* **79**, 054521 (2009).
- <sup>21</sup>G. H. Cao, S. Jiang, X. Lin, C. Wang, Y. K. Li, Z. Ren, Q. Tao, J. H. Dai, Z. A. Xu, and F. C. Zhang, arXiv:0807.4328 (unpublished).
- <sup>22</sup>A. S. Sefat, R. Jin, M. A. McGuire, B. C. Sales, D. J. Singh, and D. Mandrus, *Phys. Rev. Lett.* **101**, 117004 (2008).
- <sup>23</sup>L. J. Li, Y. K. Luo, Q. B. Wang, H. Chen, Z. Ren, Q. Tao, Y. K. Li, X. Lin, M. He, Z. W. Zhu, G. H. Cao, and Z. A. Xu, *New J. Phys.* **11**, 025008 (2008).
- <sup>24</sup>A. Leithe-Jasper, W. Schnelle, C. Geibel, and H. Rosner, *Phys. Rev. Lett.* **101**, 207004 (2008).
- <sup>25</sup>Z. Ren, Z. W. Zhu, S. Jiang, X. F. Xu, Q. Tao, C. Wang, C. M. Feng, G. H. Cao, and Z. A. Xu, *Phys. Rev. B* **78**, 052501 (2008).
- <sup>26</sup>H. S. Jeevan, Z. Hossain, D. Kasinathan, H. Rosner, C. Geibel, and P. Gegenwart, *Phys. Rev. B* **78**, 052502 (2008).
- <sup>27</sup>M. Rotter, M. Tegel, and D. Johrendt, *Phys. Rev. Lett.* **101**, 107006 (2008).
- <sup>28</sup>G. F. Chen, Z. Li, G. Li, W. Z. Hu, J. Dong, X. D. Zhang, P. Zheng, N. L. Wang, and J. L. Luo, *Chin. Phys. Lett.* **25**, 3403 (2008).
- <sup>29</sup>K. Sasmal, B. Lv, B. Lorenz, A. M. Guloy, F. Chen, Y. Y. Xue, and C. W. Chu, *Phys. Rev. Lett.* **101**, 107007 (2008).
- <sup>30</sup>H. S. Jeevan, Z. Hossain, D. Kasinathan, H. Rosner, C. Geibel, and P. Gegenwart, *Phys. Rev. B* **78**, 092406 (2008).
- <sup>31</sup>Y. P. Qi, Z. S. Gao, L. Wang, D. L. Wang, X. P. Zhang, and Y. W. Ma, *New J. Phys.* **10**, 123003 (2008)..
- <sup>32</sup>F. Izumi and T. Ikeda, *Mater. Sci. Forum* **321–324**, 198 (2000).
- <sup>33</sup>S. Jiang, Y. K. Luo, Z. Ren, Z. W. Zhu, C. Wang, X. F. Xu, Q. Tao, G. H. Cao, and Z. A. Xu, *New J. Phys.* **11**, 025007 (2009)..
- <sup>34</sup>T. Wu, G. Wu, H. Chen, Y. L. Xie, R. H. Liu, X. F. Wang, and X. H. Chen, arXiv:0808.2247 (unpublished).
- <sup>35</sup>H. Raffius, E. Mörsen, B. D. Mosel, W. Müller-Warmuth, W. Jeitschko, L. Terbüchte, and T. Vomhof, *J. Phys. Chem. Solids* **54**, 135 (1993).
- <sup>36</sup>Z. Ren, S. Jiang, S. G. Xu, H. Xing, G. H. Cao, and Z. A. Xu, (unpublished).
- <sup>37</sup>C. F. Miclea, M. Nicklas, H. S. Jeevan, D. Kasinathan, Z. Hossain, H. Rosner, P. Gegenwart, C. Geibel, and F. Steglich, arXiv:0808.2026 (unpublished).